FULL PAPER

Dalton
www.rsc.org/dalton

Versatility of the nature of the magnetic Cu(II)–U(IV) interaction. Syntheses, crystal structures and magnetic properties of Cu_2U and CuU compounds

Lionel Salmon,*[a] Pierre Thuéry,[a] Eric Rivière,[b] Jean-Jacques Girerd[b] and Michel Ephritikhine*[a]

[a] *Service de Chimie Moléculaire, DSM, DRECAM, CNRS URA 331, Laboratoire Claude Fréjacques, CEA/Saclay, 91191 Gif-sur-Yvette, France. E-mail: ephri@drecam.cea.fr*

[b] *Laboratoire de Chimie Inorganique, Institut de Chimie Moléculaire et des Matériaux, CNRS UMR 8613, Université de Paris-Sud, 91405 Orsay Cedex, France*

Received 22nd April 2003, Accepted 23rd May 2003
First published as an Advance Article on the web 12th June 2003

Treatment of $[M(H_2L^i)]$ with $U(acac)_4$ in refluxing pyridine led to the formation of the trinuclear complexes $[\{ML^i(py)_x\}_2U]$ [L^1 = *N*,*N*′-bis(3-hydroxysalicylidene)-2,2-dimethyl-1,3-propanediamine and M = Ni, Cu or Zn; L^2 = *N*,*N*′-bis(3-hydroxysalicylidene)-1,3-propanediamine and M = Cu or Zn; L^3 = *N*,*N*′-bis(3-hydroxysalicylidene)-2-methyl-1,2-propanediamine and M = Ni, Cu or Zn; x = 0 or 1]. The dinuclear compounds $[ML^3(py)U(acac)_2]$ (M = Cu, Zn) were isolated from the reaction of $[M(H_2L^3)]$ and $U(acac)_4$ in pyridine at 60 °C. The crystal structures of the trinuclear complexes are built up by two orthogonal $ML^i(py)_x$ units which are linked to the central uranium ion by the two pairs of oxygen atoms of the Schiff base ligand; the U(IV) ion is found in the same dodecahedral configuration but the Cu(II) ion coordination geometry and the Cu ··· U distance are different by passing from L^1 or L^2 to L^3, due to the shortening of the diimino chain of L^3. These geometrical parameters seem to have a great influence on the magnetic behaviour of the complexes since the Cu–U coupling in $[\{CuL^i(py)_x\}_2U]$ (i = 1, 2) is ferromagnetic while it is antiferromagnetic in $[\{CuL^3(py)_x\}_2U]$. In the compounds $[\{CuL^3(py)_x\}_2U]$ and $[CuL^3(py)U(acac)_2]$, the Cu coordination and the Cu ··· U distance are very similar, and both exhibit an antiferromagnetic interaction.

Introduction

The discovery, in 1985, of a ferromagnetic coupling in Cu_2Gd complexes[1] marked the outset of numerous studies devoted to the understanding of the exchange interaction between 3d and 4f ions and the development of molecular-based materials with controlled and tunable properties.[2] From the first investigations, the magnetic coupling between the isotropic gadolinium(III) ion and a series of spin carriers was assumed to be intrinsically ferromagnetic. This property was explained by the electron transfer from the d transition metal or free radical magnetic orbitals into the empty 5d or 6s Gd(III) orbitals, that stabilizes the ground state with the higher spin multiplicity following Hund's rule.[3] More recent results called this model in question since the sign of the Cu(II)–Gd(III) or radical–Gd(III) interaction, ferro- or antiferromagnetic, was found to depend on the nature of the ligands around the copper or gadolinium ion and/or the donor strength of the organic radical.[4–8]

Much less studies have been dedicated to 3d–4f complexes in which the lanthanide(III) ion, Ln(III), is different from gadolinium and has an orbital contribution. Since the magnetic properties of such compounds are governed by both the thermal population of the Stark components of the 4f ion and the 3d–4f interaction, the nature of this interaction could be determined by subtracting the sole contribution of the lanthanide ion, which is reflected by the magnetic behaviour of isostructural derivatives in which the paramagnetic 3d ion, *i.e.* Cu(II), has been replaced with a diamagnetic ion, *i.e.* Zn(II) or low-spin Ni(II).[9,10] Assuming that the mechanism proposed to rationalize the ferromagnetic Cu(II)–Gd(III) interaction is valid for the other magnetic lanthanide(III) ions, the 3d–4f interaction should be antiferromagnetic for the Ln(III) ions with less than seven 4f electrons, and ferromagnetic otherwise.[3,10] The magnetic properties of a series of CuLn,[9] Cu_2Ln_2,[11] Cu_3Ln_2[10,12] and FeLn[13] compounds were found not to entirely fulfil these predictions; in particular, the results reported for the Cu–Ln coupling are not consistent for the Ln(III) ions with more than half-filled f orbitals.

In the last few years, the first compounds containing both 3d and 5f ions have been isolated. Together with the challenge of their synthesis, such complexes are attractive for their magnetic properties which, by comparison with those of the 3d–4f derivatives, would reflect the greater spatial extension of the 5f orbitals. No magnetic coupling was detected in the three-dimensional network of $[K_2Mn(C_2O_4)_4U]\cdot 7H_2O$,[14] while the trinuclear complexes $[\{ML^1(py)_x\}_2U]$ revealed the antiferromagnetic Ni–U and ferromagnetic Cu–U interactions (L^1 = *N*,*N*′-bis(3-hydroxysalicylidene)-2,2-dimethyl-1,3-propanediamine).[15] Following these studies, we have prepared new trinuclear complexes of general formula $[\{ML^i(py)_x\}_2U]$ (M = Ni, Cu, Zn) by changing the diimino chain of the Schiff base ligand [L^2 = *N*,*N*′-bis(3-hydroxysalicylidene)-1,3-propanediamine; L^3 = *N*,*N*′-bis(3-hydroxysalicylidene)-2-methyl-1,2-propanediamine (Scheme 1)]; with L^3, we succeeded in isolating the first strictly dinuclear compound of paramagnetic 3d and 5f ions, $[CuL^3(py)U(acac)_2]$.[16] Here we present the synthesis,

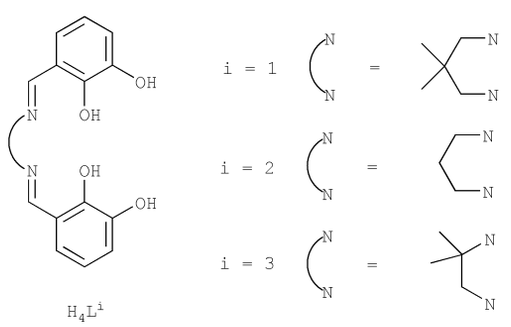

H_4L^i

Scheme 1 The H_4L^i Schiff bases.

DOI: 10.1039/b304414a

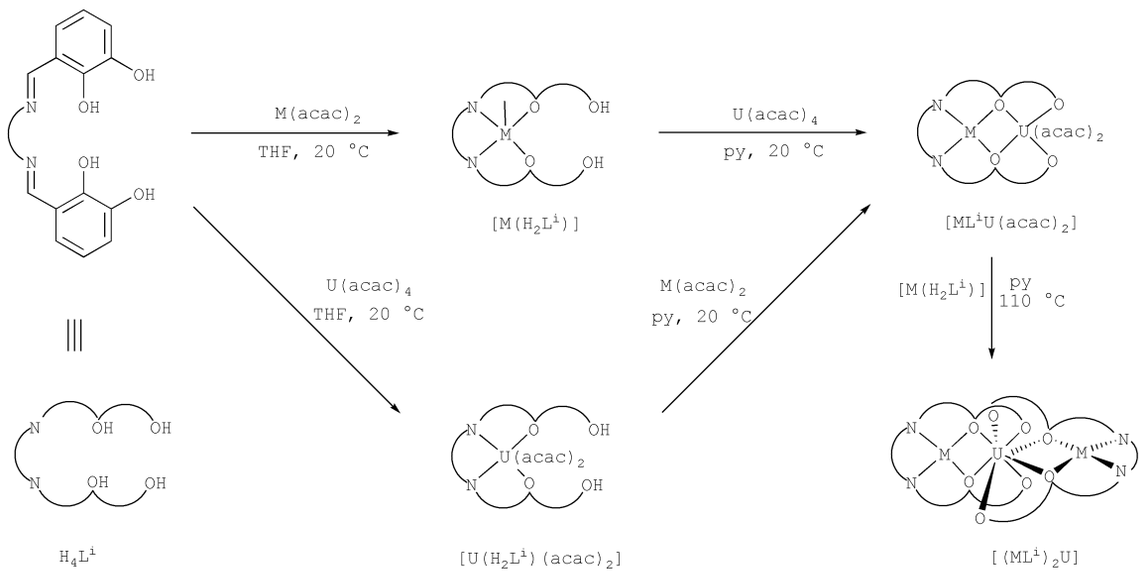

Scheme 2 Synthesis of the complexes. The pyridine ligands are not represented.

crystal structure and magnetic behaviour of these compounds. The results reveal that the Cu(II)–U(IV) interaction, like the Cu(II)–Ln(III) interaction, is strongly dependent on structural and ligand effects.

Results and discussion

Synthesis of the complexes

We recently reported that treatment of $[M(H_2L^1)]$ (M = Ni, Cu, Zn) with $U(acac)_4$ in refluxing pyridine afforded directly the trinuclear compounds $[\{ML^1(py)_x\}_2U]$, without it being possible to detect the $[ML^1(py)_xU(acac)_2]$ intermediates (Scheme 2).[15] Afterwards, we found that these latter could be observed by NMR spectroscopy when the reaction was carried out at room temperature. Thus, the Cu_2U and CuU complexes were formed in the relative proportions of 65 : 35 from an equimolar mixture of the mononuclear starting materials. Unfortunately, the dinuclear species could not be isolated pure, precluding any magnetic studies.

Similar observations were made when the Schiff base ligand L^2 was used in place of L^1. Reaction of $[M(H_2L^2)]$ (M = Cu, Zn) with 0.5 equiv. of $U(acac)_4$ in pyridine at 110 °C gave the trinuclear compounds $[\{CuL^2(py)\}U\{CuL^2\}]$ and $[\{ZnL^2(py)\}_2U]$ which were isolated as dark red and light brown crystals, in 56 and 40% yield, respectively. Here again, by lowering the temperature to 20 °C, the compound $[CuL^2(py)_xU(acac)_2]$ was formed with but was not separated from the Cu_2U complex.

Dark red crystals of $[\{ML^3\}_2U]$ (M = Cu, Ni) and orange crystals of $[\{ZnL^3(py)\}_2U]$ were obtained by treatment of $[M(H_2L^3)]$ with $U(acac)_4$ in pyridine at 110 °C, with yields higher than 80%. However, when the reaction was carried out at 60 °C, the 1 : 1 mixture of $[M(H_2L^3)]$ and $U(acac)_4$ was transformed, for M = Cu or Zn but not for M = Ni, into the dinuclear complex $[ML^3(py)U(acac)_2]$ as the sole product; the dark brown (M = Cu) and yellow (M = Zn) crystals were isolated in 55 and 73% yield, respectively. These CuU and ZnU compounds were alternatively synthesized in *ca*. 70% yield by treatment of $M(acac)_2$ with $[U(H_2L^3)(acac)_2]$. This result is not surprising in view of the better affinity of the M(II) ion for the inner N_2O_2 cavity of the Schiff base, that favoured the initial ligand exchange reaction leading to $[M(H_2L^3)]$ and $U(acac)_4$.[17] Expectedly, similar treatment of $Cu(acac)_2$ with $[U(H_2L^i)(acac)_2]$ (i = 1 or 2) gave mixtures of the CuU and Cu_2U complexes. The selective formation, under the same experimental conditions, of the M_2U compounds with the L^1 or L^2 ligands and the MU species with L^3, which likely reflects a variation in the reactivity of the U(acac) bonds in the complexes $[ML^i(py)_xU(acac)_2]$, is difficult to rationalize. However, such influence of the length of the diimino chain, $NCH_2CMe_2CH_2N$ or NCH_2CMe_2N, on the synthesis of either CuGd or Cu_2Gd compounds with a polydentate nonsymmetrical Schiff base ligand, has been previously reported.[5]

The new tri- and dinuclear compounds were characterized by their elemental analyses and X-ray crystal structure. The ^1H NMR spectra of the $[\{ML^i(py)_x\}_2U]$ complexes indicate that the Schiff base ligands L^i are equivalent; three or six resonances of equal intensities, 4H or 2H, correspond to the aromatic protons of the symmetrical L^1 and L^2 or unsymmetrical L^3 ligands, respectively, and the most shifted signals are attributed to the protons of the $CH_2N{=}CH$ fragment which are the closest to the paramagnetic 3d ion. Similar sets of resonances are observed for the L^i ligands of the dinuclear compounds $[ML^i(py)_xU(acac)_2]$. However, variable temperature studies revealed that these complexes are fluxional in solution. At 70 °C in pyridine, the acac ligands of $[CuL^3(py)_xU(acac)_2]$ give rise to two singlets in a 12 : 2 intensity ratio, indicating that all the methyl groups are magnetically equivalent. By lowering the temperature, the half-height width of the CH signal is not affected but the methyl resonance is broadened and coalescence is observed at −15 °C. Two broad signals of equal intensities (6H) are then visible at −30 °C and this slow-limit spectrum is consistent with the solid state structure of the complex (*vide infra*) which shows two equivalent acac ligands with two magnetically distinct methyl groups. The dynamic behavior of the complex, revealed by the interchange of the magnetically non equivalent Me groups of the acac ligands, can be ascribed to the facile rotation of the bidentate ligands about their U–CH axis; a similar fluxionality has been encountered in the organometallic compounds $[U(Cp)(acac)_3]$[18] and $[U(Cp)(acac)_2(OPPh_3)]$[19] (Cp = η-C_5H_5). From line shape analysis of the spectra, the free energy of activation for this process in $[CuL^3(py)_xU(acac)_2]$ is equal to 11.2(3) kcal mol^{-1}.

Crystal structure of the complexes

The crystal structures of $[\{CuL^2(py)\}U\{CuL^2\}]\cdot py$ (one of the two independent and very similar molecules), $[\{ZnL^2(py)\}_2U]\cdot 2.5py$ and $[\{CuL^3\}_2U]\cdot 1.5py$ (isomorphous with the Ni analogue) are represented in Figs. 1–3, respectively. Selected bond lengths and angles are listed in Table 1, together with those of $[\{CuL^1(py)\}U\{CuL^1\}]\cdot 2py$, $[\{ZnL^1(py)\}_2U]$ and $[\{ZnL^3(py)\}_2U]\cdot 3py$ for comparison. Hereafter, these complexes are denoted $[\{ML^i\}_2U]$, whatever the number of coordinated pyridine molecules.

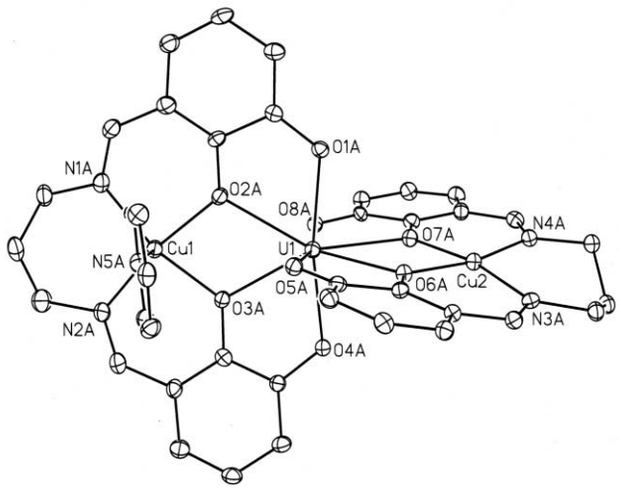

Fig. 1 View of one of the two independent molecules in the complex [{CuL^2(py)}U{CuL^2}]·py. The solvent molecule and hydrogen atoms are omitted for clarity. The displacement ellipsoids are drawn at the 10% probability level.

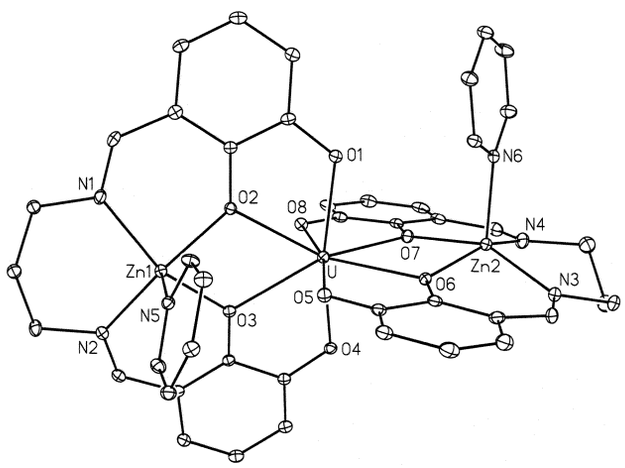

Fig. 2 View of the complex [{ZnL^2(py)}$_2$U]·2.5py. The solvent molecules and hydrogen atoms are omitted for clarity. Only one position of the disordered parts is represented. The displacement ellipsoids are drawn at the 10% probability level.

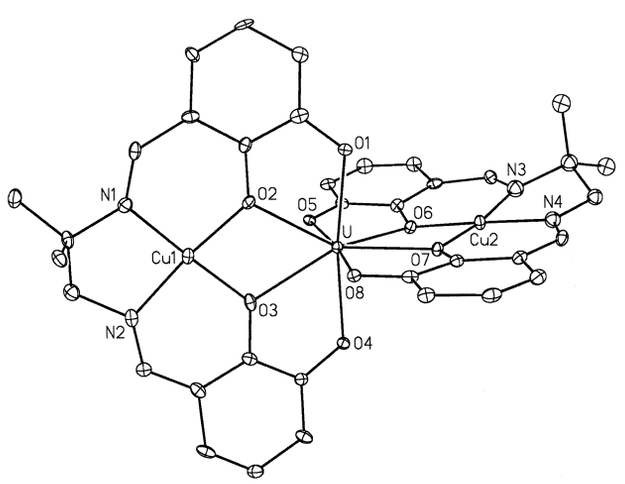

Fig. 3 View of the complex [{CuL^3}$_2$U]·1.5py. The solvent molecules and hydrogen atoms are omitted for clarity. The displacement ellipsoids are drawn at the 10% probability level.

All the trinuclear complexes are built up by two orthogonal ML^i units which are linked to the central uranium ion by the phenoxide oxygen atoms; the two pairs of oxygen atoms of the salicylidene fragments [O(2), O(3) and O(6), O(7)] are in bridging position between the 3d and 5f ions. The uranium atom is therefore in a dodecahedral arrangement defined by the two orthogonal trapezia O(1)–O(2)–O(3)–O(4) and O(5)–O(6)–O(7)–O(8). The 3d ion, which is found inside the cavity formed by the two nitrogen and two bridging oxygen atoms of the Schiff base ligand, adopts a square pyramidal or square planar coordination mode, depending on whether a pyridine molecule is attached to it or not.

For the analysis of the magnetic properties, it is necessary to compare the geometrical parameters of the trinuclear compounds with the different ligands L^i. The influence of the length of the diimino chain of the Schiff base ligand on the coordination geometry of the U atom can be assessed from the variations in the U–O distances and O–U–O angles. For a given L^i ligand, the U–O_b and U–O_t distances in the corresponding [{ZnL^i}$_2$U] and [{CuL^i}$_2$U] compounds differ at the most by 0.05 Å. Thus, the ratio of the mean U–O_b and U–O_t bond lengths, 1.02 in [{ZnL^3}$_2$U] and 1.04 in [{CuL^3}$_2$U], is smaller than the value of 1.06 measured in [{ML^i}$_2$U] (i = 1, 2; M = Cu, Zn). In what concerns the O–U–O angles, there is no variation in the O_b–U–O_b angles whereas the O_t–U–O_t angles increase by 3 or 4° by passing from L^1 or L^2 to L^3. These comparisons indicate that in the [{ML^i}$_2$U] complexes, the environment of the uranium atom is very little affected by changing M and L^i; coordination of a pyridine molecule to the 3d ion has no influence either.

In contrast, it is not surprising that the length of the diimino chain of L^i has a pronounced effect on the coordination of the 3d metal. The mean Zn–N and Zn–O distances in [{ZnL^1}$_2$U] are 0.03 Å longer than in [{ZnL^3}$_2$U]; this variation is greater, 0.06 Å, in the corresponding Cu complexes. By comparison with L^1 and L^2, the shortening of the diimino chain of L^3 induces a tightening of the N–Cu–N angles (*ca.* 10°) and an opening of the N–Cu–O and O–Cu–O angles (*ca.* 4 and 2°, respectively). In each of the three [{CuL^i}$_2$U] compounds, the sum of these angles is equal or very close to 360°, indicating that the Cu(II) ion lies in the plane of the N_2O_2 cavity, even if a pyridine molecule is attached to it. However, the inner cavity of L^i does not accommodate so perfectly the larger Zn(II) ion and its contraction, from L^1 to L^3, leads to a greater separation between this ion and the N_2O_2 plane, from 0.45(2) to 0.64(1) Å. As a consequence, for a given L^i, the N–M–N, N–M–O and O–M–O angles are smaller for M = Zn than for M = Cu, and the variations, by passing from L^1 to L^3, are greater for the N–Zn–N angles (*ca.* 14°) and smaller for the N–Zn–O and O–Zn–O angles (*ca.* 1°), by comparison with those observed for the corresponding angles in the analogous Cu compounds.

In each of the three compounds [{CuL^i}$_2$U], the dihedral angles α between the planes O_b–Cu–O_b and O_b–U–O_b are very similar and equal to 9(1) and 2(1)°. The most significant geometrical difference between the CuO_2U bridging cores, by changing L^1 or L^2 with L^3, is the shortening of the Cu ··· U distance which varies from 3.64(1) (L^1) or 3.66(1) (L^2) to 3.538(2) Å, in relation with the variations in the O_b–Cu–O_b angles (Scheme 3).

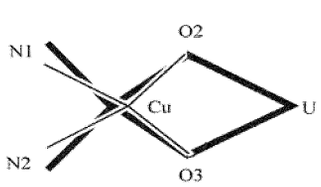

Scheme 3 Modifications in the N_2CuO_2U fragment, by passing from L^1 or L^2 (bold line) to L^3 (thin line).

The crystal structure of the dinuclear compound [CuL^3(py)-U(acac)$_2$]·1.5py is shown in Fig. 4; selected bond distances and angles in this complex and its zinc analogue [ZnL^3(py)U(acac)$_2$] are listed in Table 1. As observed in the trinuclear complexes,

Table 1 Selected bond lengths (Å) and angles (°) in the M_2U and MU complexes

	$[\{ZnL^1\}_2U]$	$[\{ZnL^2\}_2U]$	$[\{ZnL^3\}_2U]$	$[\{CuL^1\}_2U]$	$[\{CuL^2\}_2U]$ [a]	$[\{CuL^3\}_2U]$	$[\{NiL^3\}_2U]$	$[CuL^3U(acac)_2]$	$[ZnL^3U(acac)_2]$
Ref.	15	This work	16	15	This work	16	This work	16	16
U–O(1)	2.271(9)	2.315(4)	2.372(13)	2.319(6)	2.319(7); 2.295(8)	2.320(10)	2.322(12)	2.282(5)	2.305(7)
U–O(2)	2.430(8)	2.418(3)	2.400(12)	2.434(6)	2.442(6); 2.441(7)	2.395(10)	2.430(10)	2.452(5)	2.428(8)
U–O(3)	2.433(10)	2.426(4)	2.404(15)	2.433(6)	2.465(7); 2.440(8)	2.417(10)	2.446(9)	2.497(5)	2.442(7)
U–O(4)	2.311(10)	2.306(4)	2.392(13)	2.310(6)	2.301(7); 2.305(8)	2.360(10)	2.317(10)	2.264(5)	2.280(7)
U–O(5)	2.321(10)	2.317(4)	2.324(13)	2.312(6)	2.259(7); 2.272(7)	2.325(9)	2.313(9)	2.345(5)	2.404(8)
U–O(6)	2.439(9)	2.427(3)	2.402(13)	2.465(6)	2.455(7); 2.463(7)	2.448(10)	2.444(9)	2.359(5)	2.364(7)
U–O(7)	2.463(12)	2.432(4)	2.425(14)	2.453(6)	2.466(7); 2.457(7)	2.417(9)	2.436(8)	2.367(5)	2.361(7)
U–O(8)	2.325(8)	2.304(4)	2.332(13)	2.274(6)	2.291(7); 2.313(7)	2.311(9)	2.296(9)	2.359(5)	2.398(7)
<U–O>	2.37(7)	2.37(6)	2.38(4)	2.38(8)	2.37(9); 2.37(8)	2.37(5)	2.38(7)	2.37(8)	2.37(6)
<U–O_b>	2.44(1)	2.426(6)	2.41(1)	2.45(2)	2.46(1); 2.45(1)	2.42(2)	2.439(7)		
<U–O_t>	2.31(2)	2.311(6)	2.36(3)	2.30(2)	2.29(3); 2.30(2)	2.33(2)	2.31(1)		
M(1)–O(2)	2.033(9)	2.044(3)	1.985(17)	1.947(6)	1.952(7); 1.955(7)	1.862(11)	1.833(12)	1.912(5)	1.983(8)
M(1)–O(3)	2.040(12)	2.022(4)	2.032(14)	1.952(6)	1.951(6); 1.957(8)	1.867(12)	1.817(10)	1.944(5)	1.971(7)
M(1)–N(1)	2.085(12)	2.068(5)	2.03(2)	1.983(8)	1.974(9); 2.000(10)	1.897(14)	1.807(14)	1.941(7)	2.094(11)
M(1)–N(2)	2.058(12)	2.071(4)	2.12(2)	1.992(7)	2.005(11); 2.001(10)	1.930(15)	1.892(16)	1.940(6)	2.063(11)
M(1)–N(5)	2.114(13)	2.056(4)	2.023(16)	2.293(8)	2.280(10); 2.348(10)			2.320(6)	2.057(10)
M(2)–O(6)	2.016(10)	2.025(4)	1.970(12)	1.925(6)	1.912(7); 1.913(7)	1.858(10)	1.821(9)		
M(2)–O(7)	2.027(11)	2.020(4)	2.021(13)	1.912(6)	1.923(7); 1.928(7)	1.870(10)	1.818(9)		
M(2)–N(3)	2.122(12)	2.071(5)	2.044(17)	1.976(7)	1.983(7); 1.963(9)	1.933(7)	1.850(10)		
M(2)–N(4)	2.061(12)	2.071(6)	1.994(16)	1.970(8)	1.971(9); 1.962(9)	1.942(8)	1.853(9)		
M(2)–N(6)	2.03(2)	2.090(5)	2.077(15)						
M(1) ··· U	3.718(1)	3.6824(7)	3.606(3)	3.634(1)	3.6478(14); 3.6662(15)	3.536(2)	3.520(2)	3.574(1)	3.6653(13)
M(2) ··· U	3.682(1)	3.6896(7)	3.661(2)	3.648(1)	3.6709(13); 3.6607(14)	3.540(2)	3.528(2)		
O(1)–U–O(4)	167.0(3)	165.99(13)	170.8(5)	168.4(2)	169.2(2); 168.4(3)	171.8(4)	173.2(4)	163.3(2)	169.4(3)
O(2)–U–O(3)	60.6(3)	60.61(12)	61.6(6)	59.5(2)	59.3(2); 58.7(3)	58.9(4)	58.1(4)	61.2(2)	60.0(3)
O(5)–U–O(8)	165.0(4)	167.56(13)	168.7(5)	170.2(2)	169.5(2); 170.4(3)	172.1(3)	173.0(3)	146.0(2)	148.3(3)
O(6)–U–O(7)	60.8(3)	60.64(12)	60.6(4)	58.2(2)	57.3(2); 57.8(2)	58.8(3)	57.1(3)	74.2(2)	71.4(2)
N(1)–M(1)–N(2)	95.9(5)	97.76(18)	82.2(10)	97.3(3)	98.5(4); 98.9(4)	87.8(6)	87.6(7)	84.6(3)	85.0(3)
N(3)–M(2)–N(4)	97.4(5)	98.2(2)	82.2(7)	98.9(3)	99.3(4); 99.5(4)	88.6(4)	88.0(3)		
N(1)–M(1)–O(2)	88.6(4)	87.68(16)	91.1(8)	90.6(3)	91.2(4); 91.1(3)	98.8(5)	98.3(6)	95.3(3)	88.5(3)
N(2)–M(1)–O(3)	89.3(4)	89.36(17)	86.4(8)	92.9(3)	91.9(4); 91.8(4)	94.6(6)	93.2(6)	94.3(3)	90.3(3)
N(3)–M(2)–O(6)	88.5(4)	88.51(18)	92.9(6)	91.5(3)	93.5(3); 91.7(4)	97.3(3)	96.6(4)		
N(4)–M(2)–O(7)	88.2(5)	88.1(2)	88.6(6)	92.6(3)	91.7(3); 92.3(3)	94.3(3)	95.7(3)		
O(2)–M(1)–O(3)	74.1(4)	73.92(14)	75.5(6)	76.6(2)	76.9(3); 75.5(3)	78.7(5)	80.9(5)	81.6(2)	76.1(3)
O(6)–M(2)–O(7)	75.7(4)	74.65(14)	75.2(5)	77.1(2)	75.9(3); 76.5(3)	79.7(4)	79.8(4)		
M(1)–O(2)–U	112.5(4)	110.96(15)	110.3(8)	111.6(3)	111.7(3); 112.6(3)	111.7(5)	110.5(5)	109.4(2)	112.6(4)
M(1)–O(3)–U	112.1(5)	111.46(15)	108.5(7)	111.4(3)	110.8(3); 112.5(4)	110.6(5)	110.5(5)	106.5(2)	111.9(3)
M(2)–O(6)–U	111.1(4)	111.61(15)	113.3(5)	111.8(3)	113.8(3); 112.9(3)	109.8(4)	110.8(4)		
M(2)–O(7)–U	109.8(5)	111.61(16)	110.5(6)	112.8(3)	112.9(3); 112.6(3)	110.7(4)	111.2(4)		
M(1)–U–M(2)	170.9(3)	169.172(15)	168.59(6)	177.27(3)	175.92(3); 174.98(4)	173.62(5)	174.41(5)		
α_1 [b]	7.1(3)	15.4(2)	18.3(7)	8.5(2)	9.9(2); 7.6(5)	0.6(6)	0.4(6)	1.3(5)	10.8(4)
α_2 [b]	14.2(3)	10.7(3)	5.4(3)	1.7(3)	1.8(4); 3.6(4)	9.2(5)	8.6(6)		

[a] Values for the two independent molecules. [b] α_1 and α_2 are the dihedral angles between the two halves of the Cu(1)O(2)O(3)U and Cu(2)O(6)O(7)U bridging cores.

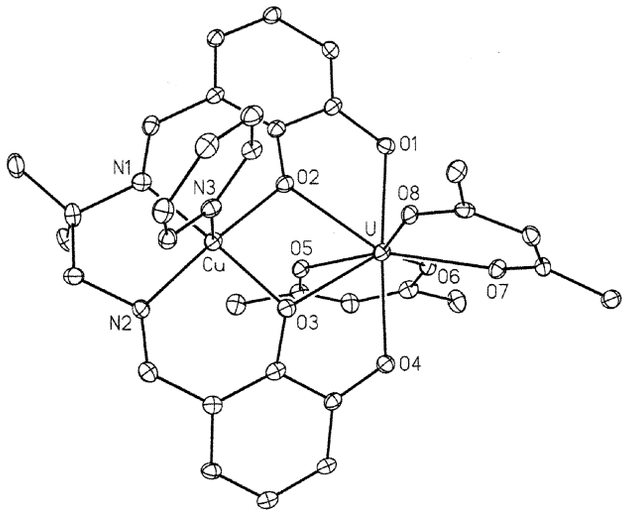

Fig. 4 View of the complex $[CuL^3(py)U(acac)_2]\cdot 1.5py$. The solvent molecules and hydrogen atoms are omitted for clarity. The displacement ellipsoids are drawn at the 10% probability level.

the Cu(II) and U(IV) ions occupy, respectively, the N_2O_2 and O_4 cavity of the Schiff base ligand and are bridged by the two oxygen atoms O2 and O3 of the salicylidene fragments. The eight oxygen atoms of L^3 and acac ligands form a dodecahedron around the U(IV) ion, the two trapezia O(1)–O(2)–O(3)–O(4) and O(5)–O(6)–O(7)–O(8) intersecting at an angle of 88.9(1)°. However, the replacement of the metalloligand CuL^3 with two acac groups causes significant variations in the U–O distances and O–U–O angles. The U–O(1), U–O(4), U–O(6) and U–O(7) bond lengths are shorter in $[CuL^3(py)U(acac)_2]$ than in $[\{CuL^3\}_2U]$, by as much as 0.1 Å, whereas the U–O(2), U–O(3), U–O(5) and U–O(8) distances are longer, by 0.05–0.10 Å. The O(1)–U–O(4) and O(5)–U–O(8) angles are smaller, by 9 and 26°, respectively, and the O(6)–U–O(7) angle is larger by 15° in the dinuclear compound. As a whole, by comparison with $[\{CuL^3\}_2U]$, the oxygen dodecahedron around the U atom in $[CuL^3(py)U(acac)_2]$ is distorted towards the square antiprism which would be defined by the two O(1)–O(2)–O(5)–O(6) and O(3)–O(4)–O(7)–O(8) faces. The coordination geometry of the U(IV) ion is the same in the structure of $[ZnL^3(py)U(acac)_2]$, the corresponding U–O bond lengths and O–U–O angles differing by less than 0.07 Å and 6°, respectively.

The square pyramidal configurations of the Cu(II) ion are slightly different in $[CuL^3(py)U(acac)_2]$ and $[\{CuL^3\}_2U]$. The Cu–N and Cu–O distances are shorter in the trinuclear complex, by *ca.* 0.03 and 0.06 Å, respectively, while the N–Cu–N, N–Cu–O and O–Cu–O angles vary at the most by a value of 3°; the Cu(II) ion is displaced from the N_2O_2 base by 0.266(3) Å towards the pyridine ligand. In the zinc analogue, the separation between the 3d metal and the N_2O_2 plane is 0.600(5) Å.

The differences between the corresponding angles of the CuO_2U bridging cores of $[CuL^3(py)U(acac)_2]$ and $[\{CuL^3\}_2U]$ do not exceed 4°. The Cu ··· U distance in the dinuclear compound is 3.574(1) Å, *i.e.* 0.04 Å longer than in the trinuclear complex.

The intermetallic Cu ··· Cu distances between two distinct molecules of the trinuclear complexes $[\{CuL^i\}_2U]$ are equal to 6.446(3) Å (L^1), 6.007(3) Å (L^2) and 5.922(4) Å (L^3); a value of 8.783(2) Å was found in the dinuclear compound $[CuL^3(py)U(acac)_2]$.

Magnetic properties of the complexes

The magnetic behaviour of the trinuclear complexes $[\{CuL^i\}_2U]$ (i = 1–3) and their zinc analogues is represented in Fig. 5 in the form of $\chi_M T$ *vs.* T. For the Zn_2U compounds, as well as for $[\{NiL^3\}_2U]$ in which the Ni(II) ion is diamagnetic, the $\chi_M T$ values represent the contribution of the sole U(IV) ion in its crystal field; they decrease with T, due to the depopulation of the Stark sublevels, to reach 0 cm^3 mol^{-1} K at 2 K since the local ground state of the U(IV) site is nonmagnetic. The curves of $\chi_M T$ *vs.* T for these Zn_2U and Ni_2U compounds are very similar, with maximum deviations of 0.15 cm^3 mol^{-1} K, in agreement with the fact that the dodecahedral configuration of the uranium atom is very similar in the trinuclear complexes.

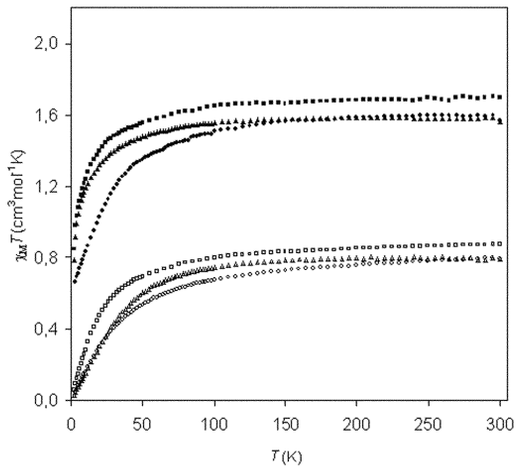

Fig. 5 Thermal dependence of $\chi_M T$ for the complexes $[\{CuL^i\}_2U]$ [L^1 (■), L^2 (▲), L^3 (●)] and $[\{ZnL^i\}_2U]$ [L^1 (□), L^2 (Δ), L^3 (○)]

The curves of $\chi_M T$ *vs.* T for the two compounds $[\{CuL^i\}_2U]$ (i = 1 or 2) are almost parallel and deviate by *ca.* 0.1 cm^3 mol^{-1} K. Between 300 and 100 K, the $\chi_M T$ products $(\chi_M T)[\{CuL^i\}_2U]$ are equal to 1.7 and 1.6 cm^3 mol^{-1} K for i = 1 or 2, respectively, and then decrease with the temperature to reach the values of 0.85 and 0.78 cm^3 mol^{-1} K at 2 K; these values are close to that expected from two noninteracting Cu(II) ions. The difference $\Delta(\chi_M T) = (\chi_M T)[\{CuL^i\}_2U] - (\chi_M T)[\{ZnL^i\}_2U]$, represented in Fig. 6, is equal to approximately 0.8 cm^3 mol^{-1} K between 300 and 100 K, then increases as T is lowered to reach a maximum value of 0.95 cm^3 mol^{-1} K (L^1) or 1.05 cm^3 mol^{-1} K (L^2), and finally drops to 0.79 or 0.75 cm^3 mol^{-1} K at 2 K. Therefore, the interaction between the Cu(II) and U(IV) ions is ferromagnetic in the two Cu_2U complexes with the L^1 and L^2 ligands, a result which was expected in the absence of any significant structural variations in these compounds.

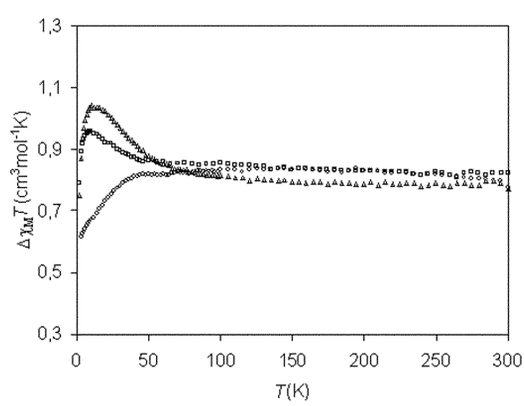

Fig. 6 Thermal dependence of $\Delta(\chi_M T) = (\chi_M T)[\{CuL^i\}_2U] - (\chi_M T)[\{ZnL^i\}_2U]$ [L^1 (□), L^2 (Δ), L^3 (○)]

However, the magnetic behaviour of $[\{CuL^3\}_2U]$ is different from that of the above Cu_2U compounds, as shown by the profile of the $\chi_M T$ *vs.* T plot. Below 100 K, the decrease of the $\chi_M T$ values is more pronounced for $[\{CuL^3\}_2U]$ than for $[\{CuL^2\}_2U]$, with the largest deviations of 0.40 cm^3 mol^{-1} K observed at about 10 K; $\chi_M T$ is equal to 0.66 cm^3 mol^{-1} K at 2 K. As a consequence, the difference $\Delta(\chi_M T) = (\chi_M T)$-$[\{CuL^3\}_2U] - (\chi_M T)[\{ZnL^3\}_2U]$ decreases with the temper-

ature, revealing that the Cu(II)–U(IV) interaction is antiferromagnetic. It is interesting to note that the values of $\chi_M T$ and $\Delta(\chi_M T)$ at 2 K are smaller by *ca.* 0.15 $cm^3\ mol^{-1}$ K to that expected from two noninteracting Cu(II) ions.

The field dependence at 2 K of the difference $\Delta M = M[\{CuL^1\}_2U] - M[\{ZnL^1\}_2U]$, M being the magnetization, closely follows the Brillouin function for two non interacting Cu(II) ions,[14] that is consistent with the value of 0.79 $cm^3\ mol^{-1}$ K for $\Delta(\chi_M T)$ at this temperature. However, the curves of ΔM for the complexes $[\{CuL^i\}_2U]$ (i = 2 or 3) do not follow exactly the Brillouin function at 2 K, showing the presence of a weak residual antiferromagnetic interaction. This feature which would be related to the lower values of $\Delta(\chi_M T)$ at 2 K for both complexes, 0.75 and 0.65 $cm^3\ mol^{-1}$ K, would reflect the presence of weak intra- or intermolecular antiferromagnetic interactions between the Cu(II) ions. It is possible that intermolecular interactions are favoured in the complexes $[\{CuL^i\}_2U]$ (i = 2 or 3) where the intermetallic Cu ··· Cu distances between two distinct molecules are *ca.* 0.5 Å shorter than in $[\{CuL^1\}_2U]$.

The distinct magnetic properties of the $[\{CuL^i\}_2U]$ complexes, ferromagnetic for L^1 and L^2 and antiferromagnetic for L^3, should not be clearly related to geometrical variations in the uranium environment, as indicated by the crystal structures. It is also noteworthy that these differences cannot be connected with the dihedral angle α between the two halves of the bridging CuO_2U network, in contrast to what was observed in a series of dinuclear CuGd compounds where the ferromagnetic interaction was found to increase by lowering the bending of the CuO_2Gd core.[20] In these Cu–Gd complexes, the magnitude of the magnetic coupling was better correlated with the angle α than with the Cu ··· Gd distance. The opposite signs of the V–Gd interactions in two dinuclear compounds was also related to the distinct α angles of the VO_2Gd cores.[21]

The main significant structural differences caused by changing the length of the diimino chain in the $[\{CuL^i\}_2U]$ complexes concern the Cu(II) ion coordination and the Cu ··· U distance which is 0.1 Å shorter in $[\{CuL^3\}_2U]$. In nitrato gadolinium complexes with nitronyl nitroxide radicals, $[Gd(radical)(NO_3)_3]$, the change from ferro- to antiferromagnetic radical-Gd coupling was found to correspond to the shortening of the Gd–O(radical) distance, by *ca.* 0.06 Å.[7,22] This feature was accounted for by the better donor strength of the more tightly bound radical which would favour the direct overlap of the magnetic orbitals of the ligand with the f orbitals, leading to antiferromagnetism, over the overlap with the s and d orbitals, leading to ferromagnetism.[6] The former of these two opposite contributions to the nature and magnitude of the exchange interaction would become more easily dominant in Cu–U complexes because of the greater spatial extension of the 5f orbitals. The change from ferro- to antiferromagnetism in the complexes $[\{CuL^i\}_2U]$ could thus be explained by the shortening of the Cu ··· U distance. However, the inverse trend was observed in a series of gadolinium compounds of general formula $[Gd(radical)(hfac)_3]$ (radical = nitronyl nitroxide or imino nitroxide radical; hfac = hexafluoroacetylacetonate) where the radical-Gd interaction becomes more antiferromagnetic as the distance between the radical and the Gd(III) ion increases.[8] These observations indicate that the sign and strength of the Cu–Gd or radical–Gd interaction cannot be simply correlated with a single geometrical parameter and is much influenced by the electronic structure of the complexes and the nature of all the ligands around the metal centres. These qualitative findings are clearly transposable to the interactions between any spin carrier and other ions of the f elements, in particular uranium.

The dependence of $\chi_M T$ as a function of T for the CuU and ZnU complexes $[ML^3(py)U(acac)_2]$ (M = Cu, Zn), with the variation of $\Delta(\chi_M T) = (\chi_M T)[CuL^3U] - (\chi_M T)[ZnL^3U]$ are represented in Fig. 7. The near perfect superimposition of the $(\chi_M T)[ZnL^3U]$ and $(\chi_M T)[\{ZnL^3\}_2U]$ curves at low temperature suggest that the modifications in the dodecahedral configuration of the U(IV) ion in the di- and trinuclear complexes has little influence on the thermal population of the Stark sublevels of this ion. The difference $\Delta(\chi_M T)$ is approximately constant from 300 to 100 K and equal to 0.40 ± 0.05 $cm^3\ mol^{-1}$ K, a value which corresponds to an isolated Cu(II) ion. Below 100 K, $\Delta(\chi_M T)$ decreases to reach the minimum of 0.30 $cm^3\ mol^{-1}$ K at 40 K, and then increases back to 0.40 $cm^3\ mol^{-1}$ K at 2 K. This profile of the $\Delta(\chi_M T)$ *vs.* T plot indicates that the Cu(II)–U(IV) interaction is antiferromagnetic. At 2 K, the field dependence of the difference $\Delta M = M(CuL^3U) - M(ZnL^3U)$ corresponds to the Brillouin function of an isolated Cu(II) ion. It is noteworthy that in the CuU and Cu_2U compounds with the L^3 ligand, which both exhibit an antiferromagnetic behaviour, the Cu coordination and the Cu ··· U distance are very similar. By considering the versatility of the 3d–4f interaction, it is clear that these first results on the magnetic coupling of a strictly dinuclear CuU compound will have to be compared with further data obtained from other structurally distinct derivatives, in order to get a satisfactory understanding and eventually to strengthen an accurate theoretical model of this interaction.[23,24]

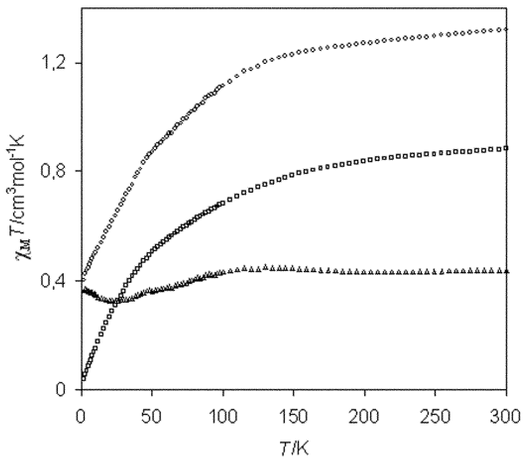

Fig. 7 Thermal dependence of $\chi_M T$ for the complexes $[CuL^3(py)U(acac)_2]$ (○) and $[ZnL^3(py)U(acac)_2]$ (□) and the difference $\Delta(\chi_M T) = (\chi_M T)[CuL^3U] - (\chi_M T)[ZnL^3U]$ (Δ)

Conclusion

These studies on the synthesis, structure and magnetic behaviour of the compounds $[\{ML^i(py)_x\}_2U]$ and $[ML^3(py)U(acac)_2]$ (M = Cu, Zn) show that the length of the diimino chain of the Schiff base ligand L^i has a strong influence on: (a) the course of the reaction of $[M(H_2L^i)]$ and $U(acac)_4$ since it is only with L^3 that it was possible to isolate the first strictly dinuclear complexes containing paramagnetic 3d and 5f ions, (b) the coordination geometry of the Cu(II) ion and the Cu ··· U distance which are different in $[\{ML^3(py)_x\}_2U]$ and $[\{ML^i(py)_x\}_2U]$ (i = 1, 2), while the U(IV) ion adopts the same dodecahedral configuration in all the trinuclear compounds, and (c) the magnetic properties of the compounds since the Cu–U interaction is ferromagnetic in $[\{ML^i(py)_x\}_2U]$ (i = 1, 2) whereas it is antiferromagnetic in the di- and trinuclear complexes with L^3. Thus, the most significant structural features to which the sign of the Cu–U coupling can be related concern the Cu(II) ion coordination and the Cu ··· U separation. These results indicate that the Cu–U interaction, like the 3d–4f interaction, is very sensitive to slight modifications of the ligands and electronic structure of the complexes.

Experimental

All reactions were carried out under argon (<5 ppm oxygen or water) using standard Schlenk-vessel and vacuum-line

techniques or in a glove box. Solvents were dried by standard methods and distilled immediately before use; deuterated pyridine (Eurisotop) was distilled over NaH and stored over 3 Å molecular sieves. The ^{1}H NMR spectra were recorded on a Bruker DPX 200 instrument and referenced internally using the residual protio solvent resonances relative to tetramethylsilane (δ 0). Magnetic susceptibility data were collected on a powdered sample of the compound with a SQUID-based sample magnetometer Quantum design MPMS5. Elemental analyses were performed by Analytische Laboratorien at Lindlar (Germany).

The Schiff bases H_4L^i (i = 1, 2, 3) were synthesized by published methods.[25] The acac compounds $M(acac)_2$ (Ni, Cu, Zn) (Aldrich) were used without purification; $U(acac)_4$ was prepared as previously reported.[26] The complexes $[M(H_2L^i)]$ (i = 1–3) and $[U(H_2L^3)(acac)_2]$ were synthesized in THF by reaction of H_4L^i with 1 equiv. of $M(acac)_2$ or $U(acac)_4$, respectively.

Preparations

$[CuL^i(py)_xU(acac)_2]$ (i = 1, 2). (a) An NMR tube was charged with $[Cu(H_2L^1)]$ (5.0 mg, 0.0124 mmol) and $U(acac)_4$ (7.9 mg, 0.0124 mmol) in C_6D_5N (0.4 ml). After 3 h at 20 °C, the spectrum of the brown–red solution showed the signals of $[\{CuL^1(py)_x\}_2U]$ and other resonances attributed to $[CuL^1(py)_x$-$U(acac)_2]$. δ_H (C_6D_5N, 23 °C) −16.98 (12H, acac), −8.91 (2H, acac), −5.60 (6H, Me), 11.44, 25.26 and 70.40 (3 × 2H, aromatic H), 107 (4H, $w_{1/2}$ = 1200 Hz, NCH_2). The Cu_2U and CuU complexes were formed in the relative proportions of 65 : 35.

(b) In a similar fashion, $[Cu(H_2L^2)]$ (5.0 mg, 0.0133 mmol) and $U(acac)_4$ (8.5 mg, 0.0133 mmol) gave a 80 : 20 mixture of $[\{CuL^2(py)_x\}_2U]$ and $[CuL^2(py)_xU(acac)_2]$. δ_H (C_6D_5N, 23 °C) −19.2 (2H, –CH_2–), −17.16 (12H, acac), −9.58 (2H, acac), 12.0, 26.21 and 72.0 (3 × 2H, aromatic H), 95 (4H, $w_{1/2}$ = 800 Hz, NCH_2).

$[\{CuL^2(py)\}U\{CuL^2\}]$. A flask was charged with $[Cu(H_2L^2)]$ (150 mg, 0.40 mmol) and $U(acac)_4$ (127 mg, 0.20 mmol) in pyridine (25 ml). The dark brown reaction mixture was heated for 12 h at 110 °C; the red powder of the Cu_2U complex was filtered off, washed with pyridine (20 ml) and dried under vacuum (120 mg, 56%). (Found: C, 44.17; H, 3.32; N, 6.78. $C_{39}H_{33}N_5O_8Cu_2U$ requires C, 43.98; H, 3.10; N, 6.58%). δ_H (C_6D_5N, 23 °C) −21.35 (4H, –CH_2–), 4.67, 16.22 and 47.47 (3 × 4H, aromatic H), 90 (8H, $w_{1/2}$ = 400 Hz, NCH_2), 424 (4H, $w_{1/2}$ = 3500 Hz, CH=N).

$[\{ZnL^2(py)\}_2U]$. This compound was synthesized by using the same procedure as for the Cu_2U analogue and was isolated as a brown powder in 40% yield. The elemental analyses are in agreement with the formula $[\{ZnL^2(py)\}_2U]\cdot 2py$. (Found: C, 49.20; H, 4.05; N, 8.90. $C_{54}H_{48}N_8O_8Zn_2U$ requires C, 49.40; H, 3.66; N, 8.54%). δ_H (C_6D_5N, 23 °C) −8.41 (4H, –CH_2–), −6.74 (8H, NCH_2), 1.55 (4H, CH=N), 5.74, 14.88 and 24.42 (3 × 4H, aromatic H).

$[\{CuL^3\}_2U]$. A flask was charged with $[Cu(H_2L^3)]$ (150 mg, 0.38 mmol) and $U(acac)_4$ (122 mg, 0.19 mmol) in pyridine (25 ml). The red reaction mixture was heated for 12 h at 110 °C; the brown powder of the Cu_2U complex was filtered off, washed with pyridine (20 ml) and dried under vacuum (190 mg, 90%). The elemental analyses are in agreement with the formula $[\{CuL^3\}_2U]\cdot$py. (Found: C, 45.63; H, 3.74; N, 6.40. $C_{41}H_{37}$-$N_5O_8Cu_2U$ requires C, 45.05; H, 3.39; N, 6.41%). δ_H (C_6D_5N, 23 °C) −8.40 (12H, Me), 4.85, 5.14, 15.93, 16.26, 45.54 and 46.14 (6 × 2H, aromatic H), 66.9 (4H, $w_{1/2}$ = 300 Hz, NCH_2).

$[\{NiL^3\}_2U]$. This compound was synthesized by using the same procedure as for the Cu_2U analogue and was isolated as a red powder in 82% yield. (Found: C, 43.29; H, 3.36; N, 5.74. $C_{36}H_{32}N_4O_8Ni_2U$ requires C, 43.05; H, 3.19; N, 5.58%). The complex could not be characterized by its ^{1}H NMR spectrum because of its insolubility in organic solvents.

$[\{ZnL^3(py)\}_2U]$. A flask was charged with $[Zn(H_2L^3)]$ (150 mg, 0.38 mmol) and $U(acac)_4$ (122 mg, 0.19 mmol) in pyridine (25 ml). The dark orange reaction mixture was heated for 12 h at 110 °C. The brown powder of the Zn_2U complex which precipitated upon addition of pentane (20 ml) was filtered off, washed with pyridine (20 ml) and dried under vacuum (180 mg, 80%). (Found: C, 48.53; H, 4.14; N, 7.08. $C_{46}H_{42}N_6O_8Zn_2U$ requires C, 47.00; H, 3.58; N, 7.15%). δ_H (C_6D_5N, 23 °C) −8.57 (4H, NCH_2), −7.45 (12H, Me), 0.19 and 0.56 (2 × 2H, CH=N), 5.16 and 13.97 (2 × 4H, aromatic H), 23.38 and 23.58 (2 × 2H, aromatic H).

$[CuL^3(py)U(acac)_2]$. (a) A flask was charged with $[Cu(H_2L^3)]$ (150 mg, 0.38 mmol) and $U(acac)_4$ (244 mg, 0.38 mmol) in pyridine (25 ml). The dark brown reaction mixture was heated for 12 h at 60 °C. The brown powder of the CuU complex which precipitated upon addition of pentane (20 ml) was filtered off, washed with pyridine (20 ml) and dried under vacuum (190 mg, 55%). (Found: C, 43.69; H, 3.92; N, 4.77. $C_{33}H_{35}N_3O_8CuU$ requires C, 43.88; H, 3.88; N, 4.65%). δ_H (C_6D_5N, 23 °C) −16.5 (12H, $w_{1/2}$ = 200 Hz, acac), −8.7 (6 H, $w_{1/2}$ = 140 Hz, Me), −7.71 (2H, $w_{1/2}$ = 18 Hz, acac), 11.24 (2H, aromatic H), 23.79 and 24.04 (2 × 1H, aromatic H), 66.0 (2H, aromatic H), 81 (2H, $w_{1/2}$ = 1600 Hz, NCH_2); δ_H (C_6D_5N, −30 °C) −26.2 and −15.7 (2 × 6H, $w_{1/2}$ = 600 Hz, acac), −13.77 (2H, $w_{1/2}$ = 18 Hz, acac), −11.0 (6H, $w_{1/2}$ = 300 Hz, Me), 12.6 (2H, aromatic H), 27.53 and 28.17 (2 × 1H, aromatic H), 79.2 (2H, aromatic H), 99 (2H, $w_{1/2}$ = 2000 Hz, NCH_2); δ_H (C_6D_5N, 70 °C) −13.40 (12H, $w_{1/2}$ = 60 Hz, acac), −6.50 (6H, $w_{1/2}$ = 90 Hz, Me), −5.08 (2H, $w_{1/2}$ = 18 Hz, acac), 10.38 (2H, aromatic H), 21.26 (2H, aromatic H), 57.37 and 57.73 (2 × 1H, aromatic H), 69 (2H, $w_{1/2}$ = 1000 Hz, NCH_2). Coalescence of the signal of the acac methyl groups occured at −15 °C.

(b) A flask was charged with H_4L^3 (200 mg, 0.61 mmol) and $U(acac)_4$ (387 mg, 0.61 mmol) in pyridine (25 ml). The reaction mixture was heated for 12 h at 60 °C and $Cu(acac)_2$ (159 mg, 0.61 mmol) was introduced into the flask. After stirring for 24 h at 45 °C, addition of pentane (20 ml) led to the precipitation of the CuU complex wich was filtered off, washed with pyridine (20 ml) and dried under vacuum (390 mg, 71%).

$[ZnL^3(py)U(acac)_2]$. This compound was synthesized in 73% yield by using the same procedure (a) or (b) as for the CuU analogue, and was isolated as a yellow powder. (Found: C, 44.01; H, 4.05; N, 4.79. $C_{33}H_{35}N_3O_8ZnU$ requires C, 43.79; H, 3.87; N, 4.64%). δ_H (C_6D_5N, 10 °C) −23.5 (3H, acac), −21.01 (6H, acac), −14.5 (3H, acac), −12.70 and −10.62 (2 × 1H, acac), −10.20 (3H, Me), −9.36 and −6.16 (2 × 1H, NCH_2), −5.35 (3H, Me), 4.15 and 4.58 (2 × 1H, CH=N), 11.72, 12.12, 25.30, 25.66, 52.40 and 52.62 (6 × 1H, aromatic H).

Crystallography

Single crystals of the complexes were obtained by crystallization from pyridine. The crystals were introduced in glass capillaries with a protecting "Paratone" oil (Exxon Chemical Ltd.) coating. The data were collected on a Nonius Kappa-CCD area detector diffractometer[27] using graphite-monochromated Mo-Kα radiation (λ = 0.71073 Å). The unit cell parameters were determined from ten frames, then refined on all data. A 180° φ-range was scanned with 2° steps during data collection, with a crystal-to-detector distance fixed to 28 mm. The data were processed with DENZO-SMN.[28] The structures were solved by Patterson map interpretation or by direct methods with SHELXS-97[29] and subsequent Fourier-difference synthesis and refined by full-matrix least-squares on F^2 with SHELXL-97.[29] Absorption effects were corrected empirically with the program

Table 2 Crystal data and structure refinement details

	[{CuL^2(py)}U{CuL^2}]·py	[{ZnL^2(py)}$_2$U]·2.5py	[{NiL^3}$_2$U]·1.5py
Chemical formula	$C_{44}H_{38}Cu_2N_6O_8U$	$C_{56.5}H_{50.5}N_{8.5}O_8UZn_2$	$C_{43.5}H_{39.5}N_{5.5}Ni_2O_8U$
M/g mol^{-1}	1143.91	1345.32	1122.76
Crystal system	Monoclinic	Triclinic	Monoclinic
Space group	$P2_1/c$	$P\bar{1}$	$P2_1/c$
a/Å	17.4972(12)	11.7915(10)	10.3441(4)
b/Å	26.2608(11)	13.6115(10)	13.4866(10)
c/Å	17.3250(13)	16.3246(10)	31.0091(15)
α/°	90	95.631(5)	90
β/°	91.654(3)	93.623(5)	90.119(4)
γ/°	90	97.892(4)	90
V/Å^3	7957.4(9)	2574.9(3)	4326.0(4)
Z	8	2	4
D_c/g cm^{-3}	1.910	1.735	1.724
μ(Mo-Kα)/mm^{-1}	5.184	4.127	4.654
Crystal size/mm	0.20 × 0.15 × 0.12	0.32 × 0.25 × 0.10	0.20 × 0.20 × 0.15
F(000)	4464	1330	2204
θ Range/°	2.7–25.7	3.0–25.7	3.0–25.7
T/K	110(2)	100(2)	100(2)
No. of data collected	53131	17748	25784
No. of unique data	14860	9029	7381
No. of "observed" data [$I > 2\sigma(I)$]	8753	7518	5849
R_{int}	0.090	0.045	0.069
No. of parameters	1099	685	548
R_1 [a]	0.060	0.037	0.070
wR_2 [b]	0.124	0.083	0.157
S	0.989	1.027	1.064
$\Delta\rho_{min}$/e Å^{-3}	−1.02	−1.03	−0.84
$\Delta\rho_{max}$/e Å^{-3}	1.37	0.72	1.40

[a] $R_1 = \Sigma||F_o| - |F_c||/|F_o|$ (observed reflections). [b] $wR_2 = [\Sigma w(|F_o^2| - |F_c^2|)^2/\Sigma w|F_o^2|^2]^{1/2}$ (observed reflections).

DELABS from PLATON.[30] Two successive carbon atoms in each of the bridges linking the imine nitrogen atoms in [{ZnL^2(py)}$_2$U]·2.5py are disordered over two sites which were refined with occupancy parameters constrained to sum to unity. In compound [{NiL^3}$_2$U]·1.5py, the diimino chain of one of the Schiff bases and its two methyl substituents are seemingly much disordered but, the different positions being unresolved, the main (or average) component only has been kept. All non-hydrogen atoms were refined with anisotropic displacement parameters, except some of the disordered ones. Some restraints on bond lengths and/or displacement parameters were applied for some atoms of disordered parts or solvent molecules. Hydrogen atoms were introduced at calculated positions, except in the disordered parts when present, and were treated as riding atoms with a displacement parameter equal to 1.2 (CH, CH_2) or 1.5 (CH_3) times that of the parent atom. In [{ZnL^2(py)}$_2$U]·2.5py and [{NiL^3}$_2$U]·1.5py, the poor resolution and consequent imperfect location of the diimino chains result in some intermolecular contacts shorter than usual. In the last compound in particular, an anomalously short contact of 2.78 Å is observed between one methyl group of the poorly resolved diimino chain and a pyridine carbon atom (affected with a 0.5 occupancy factor). Furthermore, a void of 91 Å^3 in this structure suggests the presence of another disordered solvent molecule, which could not be located from Fourier-difference maps. Crystal data and structure refinement details are given in Table 2. The molecular plots were drawn with SHELXTL.[31] All calculations were performed on a Silicon Graphics R5000 workstation.

CCDC reference numbers 208958–208960.

See http://www.rsc.org/suppdata/dt/b3/b304414a/ for crystallographic data in CIF or other electronic format.

References

1 A. Bencini, C. Benelli, A. Caneschi, R. L. Carlin, A. Dei and D. Gatteschi, *J. Am. Chem. Soc.*, 1985, **107**, 8128.

2 R. E. P. Winpenny, *Chem. Soc. Rev.*, 1998, **27**, 447; C. Benelli and D. Gatteschi, *Chem. Rev.*, 2002, **102**, 2369.

3 M. Andruh, I. Ramade, E. Codjovi, O. Guillou, O. Kahn and J. C. Trombe, *J. Am. Chem. Soc.*, 1993, **115**, 1822.

4 J.-P. Costes, F. Dahan, A. Dupuis and J.-P. Laurent, *Inorg. Chem.*, 2000, **39**, 169.

5 J.-P. Costes, F. Dahan and A. Dupuis, *Inorg. Chem.*, 2000, **39**, 5994.

6 A. Caneschi, A. Rei, D. Gatteschi, L. Sorace and K. Vostrikova, *Angew. Chem., Int. Ed.*, 2000, **39**, 246.

7 C. Lescop, E. Belorizky, D. Luneau and P. Rey, *Inorg. Chem.*, 2002, **41**, 3375.

8 C. Lescop, D. Luneau, P. Rey, G. Bussière and C. Reber, *Inorg. Chem.*, 2002, **41**, 5566.

9 J.-P. Costes, F. Dahan, A. Dupuis and J.-P. Laurent, *Chem. Eur. J.*, 1998, **4**, 1616.

10 M. L. Kahn, C. Mathonière and O. Kahn, *Inorg. Chem.*, 1999, **38**, 3692.

11 T. Kido, Y. Ikuta, Y. Sunatsuki, Y. Ogawa and N. Matsumoto, *Inorg. Chem.*, 2003, **42**, 398.

12 R. Baggio, M. T. Garland, Y. Moreno, O. Peña, M. Perec and E. Spodine, *J. Chem. Soc., Dalton Trans.*, 2000, 2061.

13 A. Figuerola, C. Diaz, J. Ribas, V. Tangoulis, J. Granell, F. Lloret, J. Mahia and M. Maestro, *Inorg. Chem.*, 2003, **42**, 641.

14 K. P. Mörtl, J.-P. Sutter, S. Gohlen, L. Ouahab and O. Kahn, *Inorg. Chem.*, 2000, **39**, 1626.

15 T. Le Borgne, E. Rivière, J. Marrot, P. Thuéry, J.-J. Girerd and M. Ephritikhine, *Chem. Eur. J.*, 2002, **8**, 774; T. Le Borgne, E. Rivière, J. Marrot, P. Thuéry, J. -J. Girerd and M. Ephritikhine, *Angew. Chem., Int. Ed.*, 2000, **39**, 1647.

16 Preliminary communication: L. Salmon, P. Thuéry, E. Rivière, J.-J. Girerd and M. Ephritikhine, *Chem. Commun.*, 2003, 762.

17 E. Solari, F. Corazza, C. Floriani, A. Chiesi-Villa and C. Guastini, *J. Chem. Soc., Dalton Trans.*, 1990, 1345.

18 A. Dormond, A. Dahchnour and C. Duval-Huet, *J. Organomet. Chem.*, 1982, **224**, 251.

19 C. Baudin, P. Charpin, M. Ephritikhine, M. Lance, M. Nierlich and J. Vigner, *J. Organomet. Chem.*, 1988, **345**, 263.

20 J.-P. Costes, F. Dahan and A. Dupuis, *Inorg. Chem.*, 2000, **39**, 165.

21 J.-P. Costes, F. Dahan, B. Donnadieu, J. Garcia-Tojal and J.-P. Laurent, *Eur. J. Inorg. Chem.*, 2001, 363.

22 J.-P. Sutter, M. L. Kahn, S. Gohlen, L. Ouahab and O. Kahn, *Chem. Eur. J.*, 1998, **4**, 571; M. L. Kahn, J.-P. Sutter, S. Gohlen, P. Guionneau, L. Ouahab, O. Kahn and D. Chasseau, *J. Am. Chem. Soc.*, 2000, **122**, 3413.

23 I. Rudra, C. Raghu and S. Ramasesha, *Phys. Rev. B*, 2002, **65**, 224411.

24 V. S. Mironov, L. F. Chibotaru and A. Ceulemans, *Phys. Rev. B*, 2003, **67**, 014424.
25 A. Aguiari, E. Bullita, U. Casellato, P. Guerriero, S. Tamburini and P. A. Vigato, *Inorg. Chim. Acta*, 1992, **202**, 157.
26 A. Vallat, E. Laviron and A. Dormond, *J. Chem. Soc., Dalton Trans.*, 1990, 921.
27 Kappa-CCD Software, Nonius BV, Delft, The Netherlands, 1998.
28 Z. Otwinowski and W. Minor, *Methods Enzymol.*, 1997, **276**, 307.
29 G. M. Sheldrick, SHELXS-97 and SHELXL-97, University of Göttingen, Germany, 1997.
30 A. L. Spek, PLATON, University of Utrecht, The Netherlands, 2000.
31 G. M. Sheldrick, SHELXTL, Version 5.1, University of Göttingen, Germany, distributed by Bruker AXS, Madison, WI, 1999.